NEAR REAL TIME PROCESSING OF DSM FROM AIRBORNE DIGITAL CAMERA SYSTEM FOR DISASTER MONITORING

F. Kurz*, V. Ebner, D. Rosenbaum, U. Thomas, P. Reinartz

German Aerospace Center (DLR), Remote Sensing Technology Institute, PO Box 1116, D-82230 Weßling, Germany - franz.kurz@dlr.de

Commission IV, WG IV/9

KEY WORDS: Digital elevation model, airborne optical camera, disaster monitoring, near real time processing

ABSTRACT:
Knowledge of accurate digital surface models (DSMs) is a valuable information for security authorities and organizations during emergencies, disasters, or big events. In this context, the potential of the recently developed digital optical camera system (3K) to derive DSMs automatically and in near real time will be evaluated. The 3K camera system with a frame rate of 3Hz consists of three non-metric off-the-shelf cameras (Canon EOS 1Ds Mark II, 16 MPixel), which are aligned in an array with one camera looking in nadir direction and two in oblique direction. The DSMs are calculated using a subpixel hierarchical matching based on interest points followed by a region growing algorithm. Exterior orientation is given online by GPS/IMU data, whereas interior camera parameters are provided in advance. The resulting DSM is calculated by forward intersection. For the validation, the point accuracies in relation to the base-to-height ratio as well as the reached point density in relation to the calculation time were calculated. Two flight campaigns with the 3K camera system were performed with varying frame rates over the centre of Munich on 30th April and on 17th June 2007. Point accuracies over flat terrain were validated with reference DEMs and correspond quite well to simulated accuracies. The validation showed that smaller base-to-height ratios decrease the point accuracies but increase point densities as images are more similar in particular over urban areas. Exemplarily possible applications for near real time DSMs in the context of disaster monitoring are described, e.g. monitoring of land slides, 3D change detection over urban area, and monitoring of infrastructure. Problematic in all cases is the long processing time, thus the matching algorithms must be modified or new techniques must be applied. Some starting points for the reduction of processing times are discussed. In this context, the proposed matching algorithms and results serve as reference for much faster implementations.

1. INTRODUCTION

1.1 Disaster monitoring

Near real time monitoring of natural disasters, mass events, and large traffic disasters with airborne SAR and optical sensors will be the focus of several projects in research and development at the German Aerospace Center (DLR) in the next years. For these applications, up-to-date ortho imagery in combination with digital surface models (DSMs) derived in near real time is a useful database for different user groups in the disaster community. One advantage of near real time DSMs is to provide 3D information to automatic image analysis tools, e.g. in particular over urban areas 3D information is useful for building change detection.
In this paper, we will focus on the generation of DSM with a newly developed digital camera system at DLR: the 3K camera system (3Kopf=3Head). This camera system broadens the spectrum of applications and also of the processing algorithms due to its ability for near real time processing onboard and due to the high frame rate of 3Hz, e.g. increased overlap in flight direction lead to more multi-ray points for DSM generation. In chapter 3 the fully automatic processing flow is described in more detail and in chapter 4 the camera system and the algorithms are validated based on several data takes over Munich. A collection of applications for near real time DSMs in the context of disaster monitoring is presented in this paper, which are in detail

- the monitoring of land slides or avalanches
- the determination of building heights
- the monitoring of urban areas (3D change detection)
- the monitoring of infrastructure

The paper ends with a discussion of procedures to shorten the processing time.

1.2 System overview

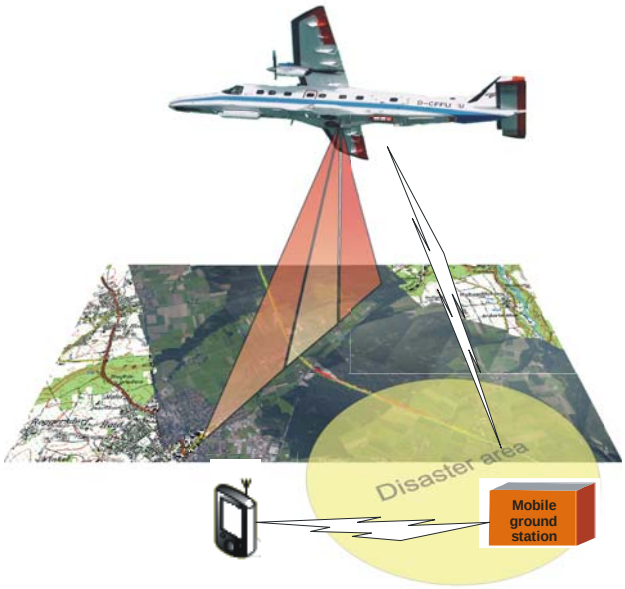

Fig 1 Airborne monitoring and processing system

For disaster monitoring from airplanes, a near real time sensor and processing system will be developed at DLR. This system consists of three digital cameras, an onboard processing unit, a microwave data link, and a mobil ground station with processing units (see Figure 1). Image data will be distributed directly to the security related ground forces in cases of disasters.
The 3K camera system consists of three non-metric off-the-shelf cameras (Canon EOS 1Ds Mark II, 16 MPix). The cameras are arranged in a mount with one camera looking in nadir direction and two in oblique sideward direction (Fig 2), which leads to an increased FOV of max *110°/ 31°* in across track/flight direction.

Fig 2 DLR 3K-camera system consisting of three Canon EOS 1Ds Mark II, integrated in a ZEISS aerial camera mount

The camera system is coupled to a GPS/IMU navigation system, which enables the direct georeferencing of the 3K optical images. Interior camera parameters were determined by a laboratory calibration (Kurz, F., 2007). Fig 3 illustrated the image acquisition geometry of the DLR 3K-camera system. Based on the use of *50 mm* Canon lenses, the relation between airplane flight height, ground coverage, and pixel size is shown, e.g. the pixel size at a flight height of *1000 m* above ground is *15 cm* and the image array covers up *2.8 km* in width.

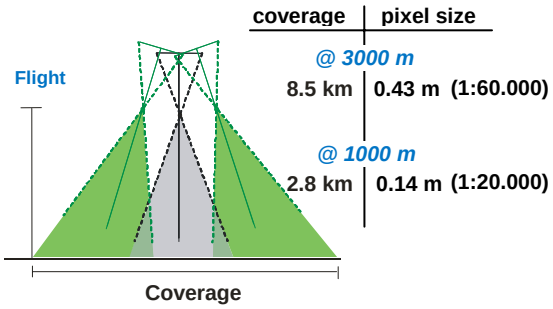

Fig 3 Illustration of the image acquisition geometry. The tilt angle of the sideward looking cameras is approx. 35°.

2. DSM GENERATION WITH 3K CAMERA SYSTEM

2.1 Automatic processing scheme for DSM generation

An overview of the automatic processing scheme for the generation of DSM using 3K imagery is given in this chapter. It is deciding that the processing flow works without user interaction fully automatic up to the DSM (see Figure 4).
Input data are three overlapping images (backward, nadir, forward) taken from the same camera. The image attitudes and positions are measured with a GPS/IMU navigation system (IGI AeroControl IId) in the differential mode with accuracies up to *0.01°/0.1m* in the real time case and up to *0.003°/0.05m* in the post-processing case. Other input data are the geometric calibration data separated in parameters of the interior orientation for each camera and the boresight alignment angles for each camera. The determination of interior orientation parameters must be done offline, whereas the estimation of boresight angles could be automated and also performed online (Kurz, F., 2007).
The most time consuming part of the DSM generation is the surface point matching (*92%* of the total processing time), which is divided into the subpixel hierarchical matching based on interest points (Lehner, M. 1992) and the subpixel region-growing matching (Heipke, C., 1996; Otto, G.P. 1989).

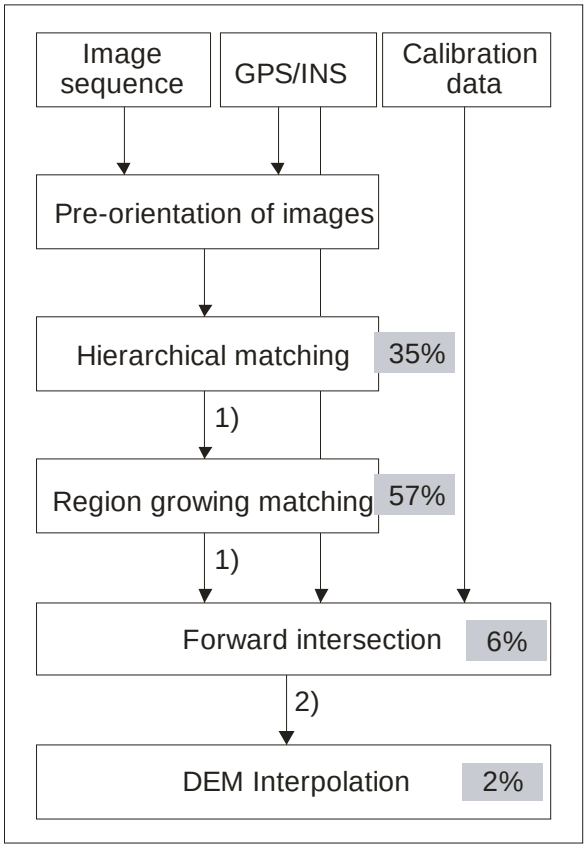

Fig 4 Automatic processing data flow for generation of DSM including calculation time in % and points filtering by 1) cross check by additional matching and by 2) outlier detection during the forward intersection.

Images must be pre-orientated to find out robust starting points for the hierarchical matching. For this, affine transformation parameters between the images are derived from GPS image positions. The hierarchical matching starts with the “Förstner” interest operator at the top of the image pyramid in the nadir image. Then, a bidirectional matching based on the normalized correlation coefficient is performed for every image pair (nadir-backward/nadir-forward). The matched points are used for the refined definition of search spaces in the next image pyramid layer, where the interest operator is performed again and the matching is repeated. The whole procedure must be repeated until the last layer of the image pyramid is reached. For the

estimation of subpixel positions, a least-squares matching is performed in the last layer given the preliminary matching points.
In the next step, a region-growing matching (Heipke, C., 1996; Otto, G.P. 1989) based on the results of the hierarchical matching is performed. The region-growing must be performed in three steps, because dense tie points in three images must be found. First, the standard bidirectional stereo region-growing is performed on the nadir-backward image pair using the tie points from the hierarchical matching as seed points. Then, the resulting tie points are searched in the forward image. Finally, the resulting 3ray tie points are cross-checked with a matching from forward to the backward image.
Given the tie points, the image positions and attitudes, as well as the calibration data, the 3D coordinates of tie points are calculated by forward intersection. Outliers could be detected in different ways. First, they are eliminated by the ratio $residue/\sigma_{residues}$ of the image coordinates in the least-squares adjustment. An advantage of using 3ray points is that outliers in the matching could be better detected than by using stereo points due to the higher redundancy. Second, outliers are filtered out by using the standard deviation of the resulting coordinates as well as by applying a value range rule.

2.2 Simulation study

Table 1 shows the expected height accuracies σ_z based on a simulation of different flight and image acquisition configurations. Accuracies for two flight heights above ground (*1000m* and *2000m*) and for four different base-to-height ratios *B/Z* from *1:5* to *1:18*, were simulated based on a varying number of images (3ray points resp. 5ray points). Given a specific flight and image configuration, the required frame rate in Hz can be derived. For the simulation, the relative accuracies of image positions and attitudes were assumed to be very high, whereas systematic deviations were not taken into account. The matching accuracy was set to *0.15* pixels.

H [m]	B/Z	σ_Z (3 images)	Hz	σ_Z (5 images)	Hz
2000	*1:5*	*0.34m*	*0.5*	*0.30m*	*0.8*
2000	*1:9*	*0.66m*	*0.9*	*0.59m*	*1.5*
2000	*1:18*	*1.33m*	*1.6*	*1.14m*	*2.7*
2000	*1:36*	*3.33m*	*3.6*	*2.97m*	*5.9*
1000	*1:9*	*0.36m*	*1.6*	*0.31m*	*2.7*
1000	*1:18*	*0.88m*	*3.6*	*0.80m*	*5.9*

Tab 1 Expected height accuracy for different configurations

The results show – as expected – best accuracies for higher base-to-height ratios and for lower flight heights, e.g. when using 3ray points from *2000m* a. G. and a base-to-height ratio of *1:5* the standard deviation is *0.34m*. In general, the standard deviation improves only by ten percent if 5ray points are used.
Nevertheless, higher base-to-height ratios cause stronger "image decorrelation" in particular in urban areas, i.e. the number of matched points increases for smaller base-to-height ratios, as e.g. similar building sides are imaged. Smaller base-to-height ratios increase on the other hand the frame rate, which could be only achieved by new digital cameras like the Canon EOS Mark II. Besides, even with a small base-to-height ratio of e.g. *1:18* and a flight height of *2000m* acceptable accuracies of *1.33m* could be reached, which are sufficient for some applications in the context of disaster monitoring.

3. PERFORMANCE RESULTS

The DSM generation processing flow was validated with 3K image data from Munich at two different flight dates. On 30th April 2007 two flight strips from *1000m* resp. *2000m* a. G., and on 17th June 2007 flight strips from *2000m* were acquired from the centre of Munich.

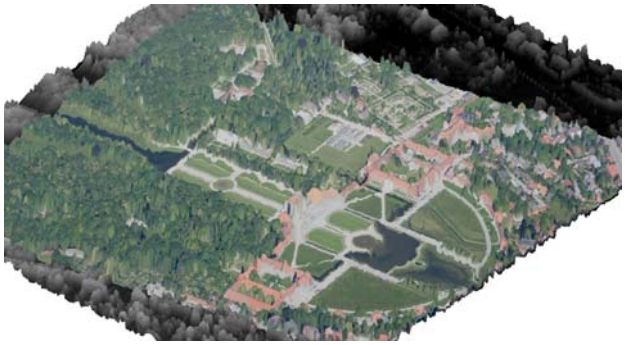

Fig 5 3K-DSM from the center of Munich: Castle Nymphenburg

The base-to-height ratio for the generation of DSM was quite small (*1:17* resp. *1:9*) because images were acquired as bursts at *1.6 Hz*. On 17th June 2007, the same area was imaged from *2000m* a. G. Here, the base-to-height ratio was higher (*1:4*), as images were acquired continuously with a low frame rate of *0.5Hz*.
3K DSMs from a reference region were generated for all flight strips according to the proposed processing flow (see example in Figure 5). All 3K DSMs were compared with a high resolution reference DEM based on LIDAR measurements.

	H [m]	B/Z (Hz)	σ_Z (sim.)	RMSE (empir.)
30/04/2007	*2000*	***1:17 (1.6)***	*1.33m*	***1.91m***
30/04/2007	*1000*	***1:9 (1.6)***	*0.36m*	***0.35m***
17/06/2007	*2000*	***1:4 (0.5)***	*0.34m*	***0.85m***

Tab 2 Accuracies of 3K DSM **over flat terrain**

Table 2 lists the simulated and empirically tested height accuracies of the processed 3K DSMs over flat terrain without vegetation and buildings. For the empirical determination of accuracies, height differences in small control areas were measured, which are not vegetated and are mostly flat.
The simulated accuracies from *1000m* a. G. (30/04/2007) correspond quite well with the empirically derived accuracies, whereas in the other flight strips the empirically derived ones were higher than in the simulation. One reason for the deviation are systematic errors, e.g. in the measured GPS coordinates, which are not included in the simulation, but produce systematic offsets in the generated 3K DSMs.
Small systematic effects could also be detected in figure 6, where histograms of the difference images, the 3K DSM minus the reference DEM, were plotted for the three data takes. Ideally, the histogram has a sharp peak at the difference zero, which could be observed e.g. in the histogram for the data take on 30th April from *1000m*. But in the other difference histograms, in particular for the data take on 30th April from *2000m*, the peak is more flat with offsets. As the difference of DSMs was calculated over urban area for every pixel, there are many reasons causing these differences. As mentioned above, systematic offset emerge from systematic errors in the D-GPS coordinates, but could emerge also from systematic differences between the LIDAR reference DEM and the 3K DSM. One

difference is that the 3K DSM contains the vegetation surface, whereas in the LIDAR reference DEM the vegetation was eliminated. Besides, in the 3K DSM generation, many errors are caused by shading effects, moving objects, surfaces with low texture, etc.

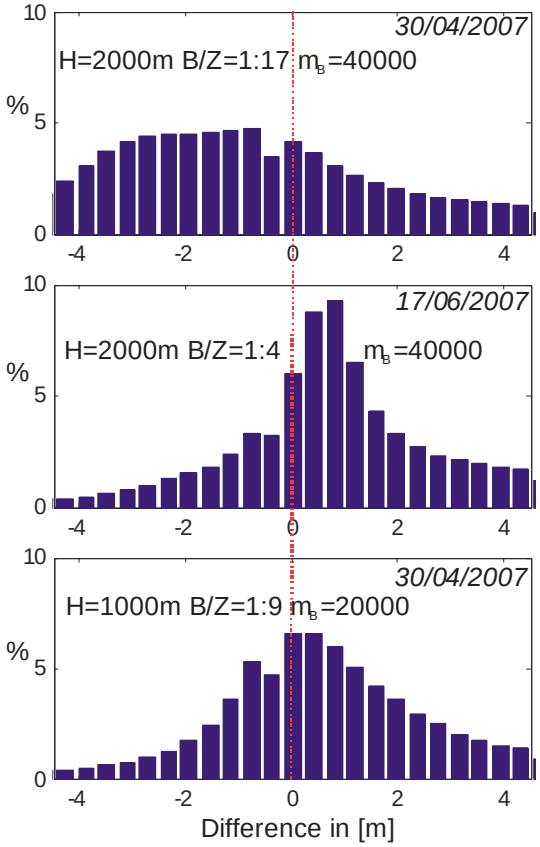

Fig 6 Histogram of DSM difference image (3K DSM minus Reference DEM) for three different data takes **over urban area**

Table 3 shows the results of the performance tests of the DSM algorithms in terms of the point density, the calculation time, and the number of outliers. From *1000m* a. G. the highest point density at *4.4* points per square meter is reached after region growing. Hence, the calculation time is also very high at together *655* minutes for a square kilometre, which is definitely too long for near real time disaster monitoring. Point density and processing time reduce with higher flight heights, e.g. from *2000m* the reached point density is only *1.35* resp. *0.65* points per square meter and the calculation time *204* resp. *241* minutes. The difference between the point densities from the *2000m* data takes is mainly caused by the "image decorrelation" over urban areas. The decorrelation is related to the base-to-height ratio, e.g. the data take on 17th June has a higher base-to-height ratio (1:4) as the data take on 30th April (1:17).
Around *4.5%* of all matching points were detected as outliers during the forward intersection. Outliers detected in the bidirectional matching before are not included in this number. The remaining outliers which were not detected are below one point per million (moving objects not included).

	H [m]	Hierarchical matching		Region growing		
		p/m^2	t/km^2	p/m^2	t/km^2	%
30/04/2007	*2000*	*0.07*	*70*	*1.35*	*134*	*4.5*
30/04/2007	*1000*	*0.19*	*250*	*4.44*	*405*	*4.6*
17/06/2007	*2000*	*0.02*	*101*	*0.65*	*141*	*4.5*

Tab 3 Performance of DSM algorithms in terms of point density [p/m^2], calculation time in minutes [t/km^2], and number of outliers in [%]

4. APPLICATIONS FOR NEAR REALTIME DSM

4.1 Monitoring of slides and avalanches

Land slides, slope failures or other movement of masses are a big natural threat in montane regions. Facing natural disasters like this, the BOS and rescue forces need detailed information about the situation in these regions, which could partly derived from remote sensing imagery.

Fig 7 The slope failure in Austria in the years 2000, 2006, and 2007

A study in the years *2006* and *2007* examined the potential of the 3K camera system to monitor a large area slope failure. Test area was Vorarlberg in Austria, where a slope failure moving fast at times during the last *150* years threads human villages. In this area, a weak layer parallel to the surface is mainly causing the natural event. The tear-off edge of the slope failure moves uphill and threads a small village above the slide. Figure 7 shows the change of the slide since the year 2000.

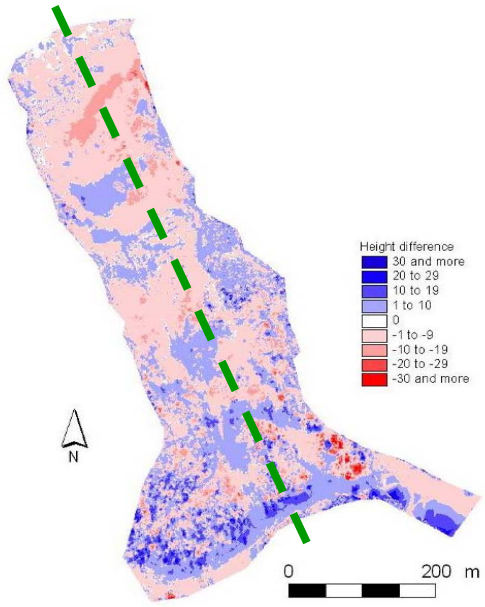

Fig 8 Difference of DSM between the years 2006 and 2007.

3K images were acquired on the 27th April 2007 in three flight strips from *1500m* to *2000m* a. G. Around 25 Ground control points were measured with GPS and reference DSMs from the years 2000, 2003, and 2006 were acquired by the Austrian cartographic office.
Using the 3K image data, a DSM of the region around the slide was generated according to the proposed processing scheme. The absolute accuracy of the DSM was validated with GCP. Thus, the accuracy of the DSM in position is around *14cm* and in the height around *40cm*. Given height variations of several meters, the accuracy is sufficient for this kind of slide.
Figure 8 shows the difference of the DSM between the 3K based DSM from the year 2007 and the DSM from the year 2006. In this case, enormous movement of masses between the two acquisition dates could be detected in the difference image. The surface height varies up to 30m.

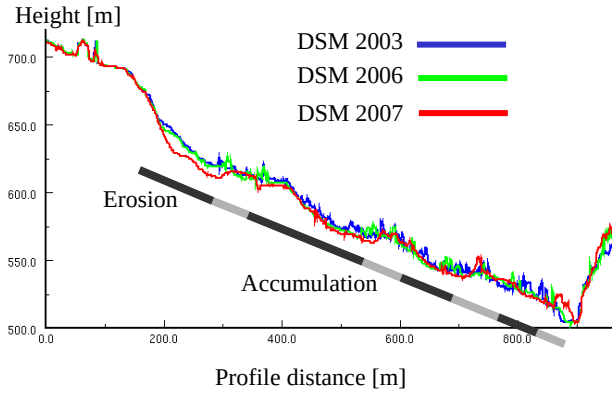

Fig 9 Profile through DSMs of the years 2003, 2006, and 2007.

The movement of the masses can be better seen in the cross section at a profile line through the whole slope (see figure 9). It could be seen, that the movement of the slide downhill is separated in different zones of erosion and accumulation, i.e. in some areas the 3K DSM from 2007 lays above or under the DSM from 2006 and 2003. Smaller variations in the surface are mainly caused by the seasonal change of the vegetation.

4.2 Determination of building heights (urban area)

The automatic determination of building heights could be useful e.g. for risk analysis before disasters or damage analysis after disasters. In this study, building heights are automatically derived from the 3K DSM supported from 3K orthoimages. A dynamic threshold operator is applied to the 3K DSM, which detects building areas. The orthoimage is used to filter out vegetation, which is falsely detected as building. In the remaining regions, the maximal difference between 3K DSM and the smoothed DSM is determined as building height. Figure 10 shows the result of the automatic building height algorithm in the center of Munich.

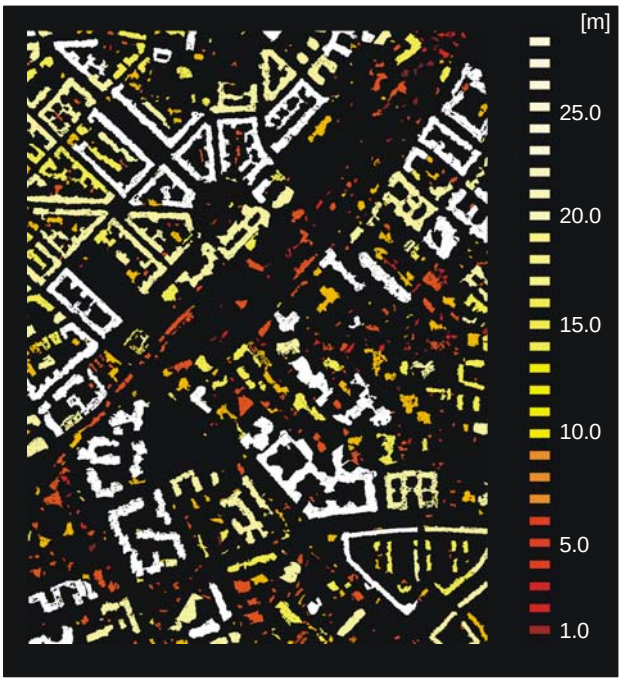

Fig 10 Automatic determination of building heights from 3K DSM

4.3 Monitoring of urban areas (3D change detection)

3D change detection in urban area is a quite helpful tool for the automatic detection of building modifications, new buildings or destroyed buildings e.g. after earthquakes.
In the airborne case and in particular for high resolution images, 3D change detection has some big advantages, e.g. a one-to-one relation between the same pixels from two different dates is prerequisite and could not be obtained in the urban area without using the 3D information.
Nevertheless, 3D change detection is a quite complex task. Problems arise not only when comparing two DSM from different sensors, like LIDAR and optical sensor. Also the comparison of two DSMs from the same sensor is quite complex, as often different faces of the buildings are exposed to the sensor, which causes variations and errors in the DSM.
First experiences with 3D change detection using DSM of 3K camera system were made with image data from 30th April and 17th June 2007 over Munich. A LIDAR reference DEM from the same area was acquired earlier by the Bavarian map authority. Flight height at both dates was *2000m* a.G. Three consecutive images were taken for DSM generation based on a height base ratio of *1:17* at 30th April and *1:4* at 17th June 2007. Figure 11 shows the difference between the 3K DSM from 17th June and the LIDAR DEM. To isolate building modifications or damages from other disturbances, morphological operations and thresholds (not discussed here) must be applied to the difference DSM. Detected 3D building changes between the acquisition dates of the DEMs are marked as red regions, e.g. the newly built Jewish Synagogue (left) and the “Schrannenhalle” (right) in the center of Munich.

4.4 Monitoring of infrastructure

Up-to-date information about the state of infrastructure, in particular about the roads, is important information for BOS after disasters. Mostly, this information can be derived directly from the images, but in some cases the 3D information could be helpful. In combination with a road data base, automatic tools

could detect e.g. bridges or bridge damages using the georeferenced image and the 3D information from the DSM. Figure 12 shows an example where the road database provides not enough information about the existence and the position of the bridge (blue lines). Automatic image tools could detect the position of the bridge more robustly together with the 3D information from the 3K DSM.

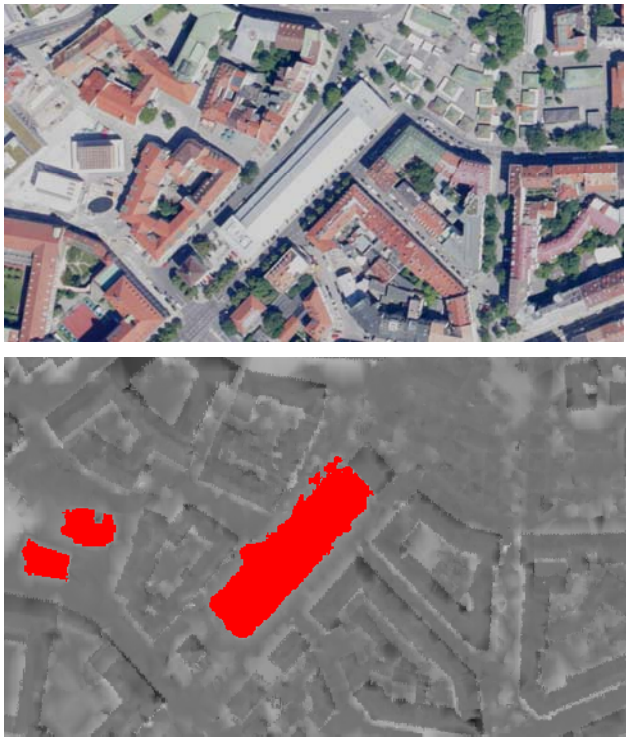

Fig 11 Difference between the 3K DSM from 17th June 2007 and the LIDAR DEM (bottom) and the corresponding orthophoto (top).

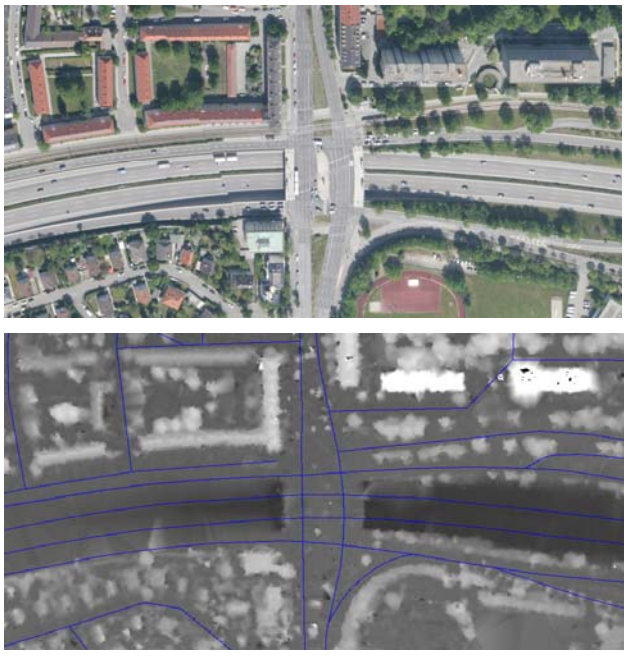

Fig 12 DSM of bridge with road data base segments (bottom) and Orthophoto (top)

5. DISCUSSION AND OUTLOOK

The 3K camera system was proved to be a robust and accurate tool for the automatic generation of DSMs. The generation of DSMs was performed with a hierarchical based matching followed by region growing algorithm. In particular for disaster monitoring, the results respective to the reached accuracy, the outlier detection, and the point density were quite satisfying as demonstrated in four applications. The main bottleneck of the DSM generation is the processing time in particular of the matching, which proved to be too long for this kind of applications based on our implementation.

A lot of progress has been made in the last years to speed up the matching algorithms. By using programmable 3D hardware, e.g. graphic processing units, the processing time for matching reduces drastically, e.g. for *512x512* pixels stereo epipolar patches the processing time is *32ms* (Zach 2004). Different techniques for fast matching using the OpenGL interface were developed, e.g. space sweeping (Bauer 2006) or mesh-based stereo algorithms (Yang 2003). Currently, tools for non epipolar images and color matching are under development.

Future work will be the integration of ideas to speed up the generation of DSMs for disaster monitoring applications.

ACKNOWLEDGEMENT

The authors would like to thank Rolf Stätter from the German Aerospace Center (DLR) and Alexandra Kollmeier from the University Munich for their support in the validation of digital elevation models.

REFERENCES

Bauer, J., Zach, C., Karner, K., 2006. Efficient Sparse 3D Reconstruction by Space Sweeping. *Technical Report VR-VIS*, Graz, Austria.

Heipke, C., 1996. The Evaluation of MEOSS Airborne Three-Line Scanner Imagery: Processing Chain and Results. *Photogrammetric Engineering & Remote Sensing*, Vol. 62, No 3, pp 293-299.

Kurz, F., Müller, R., Stephani, M., Reinartz, P., Schroeder, M. 2007. Calibration of a wide-angle digital camera system for near real time scenarios. In: *ISPRS Hannover Workshop 2007, High Resolution Earth Imaging for Geospatial Information*, Hannover, 2007-05-29 - 2007-06-01, ISSN 1682-1777

Lehner, M., Gill, R.S. 1992. Semi-automated derivation of digital elevation models from stereoscopic 3-line scanner data. *Proceedings of Satellite Symposia 1&2 from the International Space Year* Munich, Germany, 30 March – 4 April 1992.

Otto, G.P., Chau, T.K.W., 1989. 'Region growing' algorithm for matching of terrain images. *Image and Vision Computing*, 7(2): 83-92.

Yang, R., Pollefeys, M. 2003. Multi-resolution real-time stereo on commodity graphics hardware. In *Conference on Computer Vision and Pattern Recognition*.

Zach, C., Karner, K., and Bischof, H. 2004. Hierarchical disparity estimation with programmable 3D Hardware, *International Conference in Central Europe on Computer Graphics, Visualization and Computer Vision*